Temporal memory and its enhancement by estradiol requires surface dynamics of hippocampal CA1 NMDA receptors

Alice Shaam Al Abed, Mylène Potier, F Georges, Laurent Brayda-Bruno, Laurent Ladépêche, Valérie Lamothe, Shaam Al Abed, Laurent Groc, Aline Marighetto

Title page

Temporal memory and its enhancement by estradiol requires surface dynamics of hippocampal CA1 NMDA receptors

Mylène Potier PhD[1,3#], François Georges PhD[2,3#], Laurent Brayda-Bruno PhD[1,3], Laurent Ladépêche PhD[2,3], Valérie Lamothe BS[1,3], Shaam Al Abed PhD[1,3], Laurent Groc PhD[2,3*] and Aline Marighetto PhD[1,2*]

[1]Neurocentre Magendie, Physiopathologie de la Plasticité Neuronale, U862 INSERM, 146 rue Léo Saignat, 33077 Bordeaux, France; [2]Interdisciplinary Institute for NeuroSciences, CNRS UMR 5297, 33077 Bordeaux, France ; [3]Université de Bordeaux, 33077 Bordeaux France.

# These authors equally contributed to this work

* These authors share seniority

Correspondence should be addressed to: Dr. Aline Marighetto

A. Marighetto, Equipe Physiopathologie de la Mémoire Déclarative; Neurocentre Magendie Unité INSERM U862; 146 rue Léo Saignat; 33077 Bordeaux Cedex, Tel: +33 (0)5 57 57 37 17; Fax: +33 (0)5 57 57 36 69; email: aline.marighetto@inserm.fr

Keywords: Estrogen; lateral diffusion; long-term potentiation; temporal associations; episodic memory.

Words in abstract : 177 ; **Words in article body** : 3475; **Figure**s: 6 ; **Tables**: 0; **Supplemental information**: 1

Short title: NMDAR surface dynamics, estradiol and memory

Abstract

Background: Identifying the underlying cellular mechanisms of episodic memory is an important challenge since this memory, based on temporal and contextual associations among events, undergoes preferential degradation in aging and various neuropsychiatric disorders. Memory storage of temporal and contextual associations is known to rely on hippocampal NMDA receptor (NMDAR)-dependent synaptic plasticity, which depends *ex vivo* on dynamic organization of surface NMDAR. Whether NMDAR surface trafficking sustains the formation of associative memory remains however unknown. **Methods:** We here tested this hypothesis, using single nanoparticle imaging, electrophysiology and behavioral approaches in hippocampal networks challenged with a potent modulator of NMDAR-dependent synaptic plasticity and memory, 17β-estradiol (E2). **Results:** We demonstrate that E2 modulates NMDAR surface trafficking, a necessary condition for E2-induced potentiation at hippocampal CA1 synapses. Strikingly, CA1 NMDAR surface trafficking controls basal and E2-enhanced mnemonic retention of temporal, but not contextual associations. **Conclusions:** NMDAR surface trafficking and its modulation by the sex hormone E2, is a cellular mechanism critical for a major component of episodic memory, opening a new and non-canonical research avenue in the physiopathology of cognition.

Text

INTRODUCTION

NMDA receptor (NMDAR)-dependent synaptic plasticity is thought to be the basis for information storage including the formation of long-term episodic memory, our capability to remember conjunctions of *what happened, when and where* (1). In this line, it has been reported that NMDAR located in the CA1 subfield of the hippocampus, critical structure for episodic memory, are needed for long-term mnemonic retention of spatial/contextual (2) and temporal associations (3, 4). However, the implication of hippocampal NMDAR in long-term associative memory is still matter of questioning (5) and better understanding of the mechanisms by which these receptors may sustain memory is needed.

In hippocampal cultured neurons and slices, NMDAR are dynamic at the membrane surface, exploring both extrasynaptic and synaptic compartments (6-8). Moreover, NMDAR surface trafficking tunes the plasticity of maturing glutamate synapses through the fine regulation of intracellular kinase trafficking (8). Thus, NMDAR surface trafficking is an efficient mechanism to sustain synaptic plasticity and potentially associative memory formation, although this emerging possibility remains an open question.

One of the most potent physiological regulators of NMDAR-dependent plasticity and memory in the hippocampus is the sex hormone 17β-estradiol (E2; for review, 9). In various hippocampus-dependent learning tasks, performance varies as a function of the estrous cycle in females and can be enhanced by exogenous E2 (10-13). Furthermore, in both males and females, E2 is produced within the hippocampus (14), which expresses moderate levels of estrogen receptors (ER)α and ERβ (15, 16) and displays a robust response to E2. In the CA1 area, E2 modulates multiple aspects of morphological and functional synaptic plasticity, including dendritic spine density and long-term potentiation (LTP)/depression (LTD) of glutamate synapses, in a direction beneficial to mnemonic storage (17-22). At the molecular level, E2 increases NMDAR agonist binding, sensitivity to NMDAR-mediated synaptic inputs and GluN2B-NMDA excitatory post-synaptic currents (23-25). In addition, E2-induced GluN2B-NMDAR current potentiation does not result from changes in NMDAR subunit expression levels or phosphorylation status (26), but could potentially be mediated by a surface redistribution of the GluN2B-NMDAR in the perisynaptic

area, as such an effect was previously observed in aged rats (27). Collectively, these studies support the possibility that E2 may impact NMDAR synaptic plasticity and memory through a modulation of the NMDAR surface dynamics in the hippocampus.

Here, we test the hypothesis that hippocampal CA1 NMDAR surface dynamics plays a role in associative memory and its modulation by E2. We used antibodies directed against extracellular epitopes of the NMDAR, to interfere with the receptor surface trafficking without altering other intrinsic properties as previously shown (8) *in vitro* and *ex vivo* in hippocampal preparations. Using a combination of single nanoparticle imaging, electrophysiology and behavioral testing, we provide direct evidence that E2 regulates NMDAR surface dynamics and this mechanism is a necessary condition for E2-induced *in vitro* and *in vivo* hippocampal synaptic plasticity and for the temporal component of basal and E2-enhanced associative memory.

METHODS AND MATERIALS

A detailed description of all methods and materials can be found in the Supplemental Information (SI) file.

Cell culture, protein expression, synaptic live staining, immunocytochemistry, single particle (Quantum dot, QD) tracking and surface diffusion were performed in live hippocampal neurons from 18 days-old rat embryos. Surface GluA1 or GluN2A and GluN2B subunits containing NMDAR staining was performed, imaged and analyzed. Spine density, receptor surface staining, average intensity and area of fluorescently labeled surface receptor were measured within dendritic fields. GluN2A and -2B subunits containing NMDAR surface dynamics were examined after 15 min or 24 h. To affect the surface diffusion of NMDAR, we used the cross-link (X-link) procedure (figure 2G) adapted from previous published studies (28, 29).

In vivo studies were performed on 3-4 month-old C57Bl/6J naive male mice. Field excitatory postsynaptic potentials (fEPSP) evoked by stimulation of CA3 input in CA1 synapses were recorded, amplified, filtered, digitized and analyzed. NMDAR surface mobility was blocked using the X-link

protocol 45 minutes before HFS (1 train of 1s at 100 Hz) or CA1 infusion of E2 (17β-estradiol, 10 nM, 60 nL, figure 3A). Surgery and intra-hippocampal infusions in freely moving mice were performed as described previously (30, 31), (figures 4A, 5A and S1). The fear-conditioning task was conducted as described previously (31). Independent groups of mice were trained either with a 20 s interval between the tone and the shock (20 s; *trace* condition) or with the 2 stimuli contiguous (0 s; *delay* condition) (32) (figures 4A and S1). Freezing behavior was used as an index of fear responses (33). The object location task was performed as described previously (34) with minor modifications. General locomotor activity and time spent exploring each object was measured during the *acquisition* and the *test* phase after 24 h (figure 5A). Histological control of *cannulae* placements after behavioral testing was used as exclusion criteria. To check for intra-hippocampal X-link diffusion, anti-GluN1 was infused 45 min prior to sacrifice and immunohistochemistry on brains sections were performed using only secondary antibody (figures 4B and S1). All quantitative data are expressed as mean±sem. Statistical analyses performed are detailed in the SI file and in figure legends. Statistical comparisons are indicated as *, ** and *** for $p<0.05$, $p<0.01$ and $p<0.0001$, respectively.

RESULTS

E2 increases dendritic spine density, potentiates synaptic AMPAR and modulates surface NMDAR distribution in hippocampal neurons.

Since E2 is known to enhance dendritic spine density and promote hippocampal LTP, we first tested in our experimental conditions, *i.e.* cultured hippocampal neurons, that E2 induces morphological changes associated with plasticity. We measured dendritic spine density and size, as well as surface glutamate receptors density and distribution using immunocytochemistry. As expected from previous studies (24, 35-39) hippocampal neurons exposed to E2 (10 nM, 24 h) exhibited an increase in the density of dendritic spines containing post-synaptic density (PSD), labeled either with the scaffold protein Homer 1c (Figure 1A, top panel; +48.1±6.4% t_{57}=5.781; $p<0.0001$; n=32 vehicle and n=27 E2 dendritic fields) or

Shank (+28.1±2.7% t_{194}=8.125;p<0.0001; n=92 vehicle and n=104 E2 dendritic fields), reaching an average 32.4±3.9% increase without any detectable effect on the spine size (figure 1B, upper left). In addition, E2 treatment increased the surface GluA1-AMPAR content in the synaptic and extrasynaptic compartments (figures 1A-B, bottom panel and histograms). We next explored whether E2 regulates endogenous NMDAR surface distribution by focusing our attention on the two most expressed NMDAR subunits in the hippocampus, the GluN2A and GluN2B subtypes. E2 did not alter the global surface content of either of these subunits (GluN2A: +25.1±12.5%; p=0.1301; GluN2B: -0.3±3.2%; p=0.1204) but it altered their synaptic contents, increasing GluN2A-NMDAR and decreasing GluN2B-NMDAR synaptic content respectively to 183.7±25.0% and 80.9±4.6% relative to vehicle (figures 1C-D). Altogether, these data indicate that E2 increases spine density and potentiates synaptic GluA1-AMPAR. Quite remarkably, E2 redistributes surface GluN2A- and GluN2B-NMDAR in the same time window, therefore altering their synaptic ratio and possibly their related signaling.

E2 modulates GluN2-NMDAR surface trafficking, a process necessary for E2-induced increase in spine density *in vitro*

To investigate the cellular mechanism responsible for the E2 effects on GluN2-NMDAR synaptic content, we used the single nanoparticle (Quantum Dot, QD) imaging approach to track surface GluN2A- and GluN2B-NMDAR in live hippocampal neurons. We first examined the acute effect of E2 on GluN2A- or GluN2B-NMDAR surface dynamics (10 nM, 15 min; figures 2A-C). While E2 does not affect GluN2A-NMDAR, it decreases GluN2B-NMDAR surface diffusion and increases its synaptic dwell-time (time spent in the PSD area; figure 2C), leading to an overall decreased synaptic GluN2A/GluN2B ratio.

Since a 24 h treatment with E2 increases the spine density and potentiates synapses (figure 1), we next investigated the associated dynamic rearrangement of surface NMDAR. After 24 h exposure, E2 reduces GluN2A-NMDAR and enhances GluN2B-NMDAR surface diffusion (figures 2D-F). The GluN2A-NMDAR cumulative distribution of the membrane diffusion coefficient was significantly shifted, the relative fraction of immobile receptors (diffusion coefficient <0.005 $\mu m^2/s$) was increased from 52% to 75%

(figure 2E) and consistently the synaptic dwell-time was increased by 29% (data not shown). On the opposite, E2 increased membrane diffusion coefficient and mobile fraction of GluN2B-NMDAR receptors (figure 2E) and decreased the synaptic dwell-time of 18% (data not shown). Thus, E2 acutely decreases synaptic GluN2B-NMDAR surface dynamics and GluN2A/2B synaptic ratio, but after 24 h exposure, when E2-induced synaptic potentiation/spinogenesis has occurred, strong anchoring of GluN2A-NMDAR and lateral displacement of synaptic GluN2B-NMDAR, *i.e.* high synaptic GluN2A/ GluN2B ratio, is observed. This observation prompted us to test whether this surface redistribution of GluN2-NMDAR plays an instrumental role in E2 effects on the glutamate synapse adaptation. For this purpose, we artificially reduced the surface GluN2A- and GluN2B-NMDAR trafficking using an antibody-based cross-linking protocol (8, 28, 29) (figure 2G). Remarkably, both GluN2A- and GluN2B-NMDAR cross-links (X-link) fully prevented E2 effect on spine density (figures 2H-I). These data provide thus the first demonstration that GluN2A/B-NMDAR surface dynamics is required for E2 to mediate its regulatory action on the spine number in cultured hippocampal neurons.

GluN1-NMDAR surface X-linking impairs electrically- and E2-induced potentiation of CA1 synapses *in vivo*

To further explore the striking interplay between hippocampal NMDAR dynamics and synaptic adaptations, we tested the impact of interfering with surface NMDAR trafficking on two different protocols of hippocampal synaptic potentiation. *In vivo* electrophysiological recordings of fEPSP evoked by stimulation of CA3 input in CA1 synapses were performed in anesthetized mice (figures 3A-B). We first established the NMDAR-dependent LTP paradigm by controlling that i) basal fEPSP were abolished by the AMPAR antagonist, CNQX (figure 3C), ii) high frequency stimulation (HFS, 1 s, 100 Hz) induced a long-lasting enhancement of fEPSP (+160.3±38.7% compared to baseline) and iii) this LTP was completely blocked by NMDAR antagonists pre-treatments (-37.7±8.8% and -11.1±5.3% compared to baseline for AP5 and MK801, respectively; figure 3D).

Since GluN2A-NMDAR and GluN2B-NMDAR surface dynamics is required for E2-mediated action on the spine density, to interfere with surface trafficking of all NMDAR subtypes, we infused locally into hippocampal CA1, the GluN1-NMDAR X-link, as previously described (8). When injected alone, GluN1 X-link did not alter basal synaptic transmission (figure 3E) but it completely prevented the HFS-induced LTP (figure 3F). When GluN1 X-link was injected in combination with E2 into hippocampal CA1, it prevented the long-lasting potentiation of synaptic transmission evoked by E2 alone (figure 3G). Thus, NMDAR surface trafficking is a physiological mechanism contributing to *in vivo* synaptic plasticity since it is required for HFS- and E2-evoked potentiation of CA1 synaptic transmission.

Reducing NMDAR surface dynamics in the CA1 area selectively impairs temporal associative memory and its enhancement by E2.

To demonstrate the implication of local surface NMDAR trafficking in CA1 NMDAR-dependent associative memory, we used a classical *trace* fear conditioning procedure (figure 4A). This task enables assessment of both temporal and contextual fear memories, based on associations of the shock with the tone (20 s interval) and with the surrounding cues of conditioning context, respectively. We used low or high electric foot-shock intensity (0.3 and 0.6 mA) to induce weak or strong associative memories, respectively. Restricting NMDAR surface trafficking by intra CA1-infusions of GluN1 X-link (figure 4B) before a conditioning normally leading to strong fear memories (0.6 mA) has no effect on the acquisition of the fear conditioning, (figure 4C), but selectively impairs the retention of temporal associative memories (figures 4D-E). When GluN1 X-link was infused into the whole dorsal hippocampus, instead of dorsal CA1, before conditioning (figures S1A-B), it impairs acquisition of fear conditioning (figure S1C) and both retention of temporal and contextual associative memories (figures S1D-E), whereas, infusion into the Dentate Gyrus (DG) does not impair neither acquisition nor retention of the tone and context (see supplemental results, SI file). Taken together, these findings indicate selective involvement of CA1 NMDAR surface trafficking in the temporal component of associative memory.

To provide further evidence supporting this functional selectivity, we performed intra CA1-infusion of GluN1 X-Link in another typical hippocampal dependent-task with no requirement for temporal association, the object location task (34, 40). As expected, restricting NMDAR surface trafficking by intra CA1-infusion of GluN1 X-link (figure 5A) spares both the acquisition and the retention (figures 5B-C; table S1) of object location memory. Overall, our results show that CA1 NMDAR surface trafficking is required during learning to form long-term memory of temporal, but not contextual associations.

To further demonstrate the implication of CA1 NMDAR surface trafficking in the formation of long-term associative memory, we examined whether this trafficking was required for associative memory modulation by E2 using combinations of intra-CA1 infusions of vehicle/E2 and control/GluN1 X-link before conditioning. As we expected E2 to enhance memory retention, conditioning was performed under the low shock intensity condition (0.3 mA), normally leading to weak fear memories. In addition to *trace* conditioning, we also used the *delay* conditioning procedure (*i.e.*, 0 s tone-shock interval) evaluating elementary fear memory, to further assess selectivity of GluN1 X-link effects for the temporal component of associative memories (figure 6). We found that E2 enhanced the retention of both temporal and elementary fear memories and that only the enhancement of temporal memory was prevented by GluN1 X-link (figures 6A-B). While in *trace* or *delay* conditioning, neither the acquisition of conditioning (data not shown) nor contextual memory retention (figures 6C-D) were modified by E2 and/or GluN1 X-link (figures 6C-D).

Altogether, our findings indicate that NMDAR surface trafficking in hippocampal CA1 is a critical mechanism in the formation of long-term fear memories based on associations across time and their enhancement by E2.

DISCUSSION

We here provide the first demonstration that NMDAR surface trafficking in the dorsal CA1 of the hippocampus is a crucial cellular mechanism for long-term plasticity of glutamate synapse and contributes to certain NMDAR components of associative memory and their modulation by E2 in the

adult rodent. Using a X-linking procedure that restricts NMDAR surface mobility without altering other intrinsic receptor properties (8) and a set of high-resolution live imaging, *in vivo* electrophysiology and behavioral testing, we demonstrate that i) E2 regulates the surface trafficking of GluN2A- and GluN2B-NMDAR, ii) NMDAR surface dynamics is required for E2-induced increase in spine density, HFS- and E2-induced LTP of CA1 synapses and iii) NMDAR surface dynamics in the dorsal CA1 is required for 24 h mnemonic retention of temporal associative fear memory and its enhancement by E2, but is not necessary for contextual and elementary fear memories. This study sheds a new light on the key role of NMDAR cellular distribution in memory since it indicates that the NMDAR surface dynamics and not only the channel activity *per se* (8, 41) regulates the LTP of glutamate synapses *in vitro* and *in vivo* and, in CA1, sustains the formation of long-term memory of associations across time, an important component of episodic memory (42).

The regulation of NMDAR signaling and NMDAR-dependent synaptic plasticity by E2 has long been reported (9, 43). We here show that E2 increases AMPAR synaptic content and dendritic spine density through a surface redistribution of the two key GluN2A- and GluN2B-NMDAR subtypes in hippocampal neurons. Acutely, E2 rapidly increases the synaptic anchoring of GluN2B-NMDAR without notably changing GluN2A-NMDAR surface trafficking. This effect is transitory since after 24 h of E2 exposure, when synaptic AMPAR contents and spine density are already and stably increased, we reported an increased synaptic GluN2A/2B ratio. The description of the regulated NMDAR membrane dynamics supports the well-established enhancing effects of E2 on various forms of hippocampal NMDAR-dependent LTP (reviewed in 44). The acute change in GluN2B-NMDAR surface trafficking leading to reduced synaptic GluN2A/2B ratio was predictive of a LTP induction facilitation at excitatory synapses (45, 46). This suggestion is supported since an *in vivo* intra-hippocampal infusion of E2, at a physiological dose (14), acutely potentiates CA3-CA1 synaptic transmission (see also, 25) in a surface NMDAR trafficking-dependent manner. In line with the present findings, E2 has been shown to enhance GluN2B-dependent excitatory postsynaptic currents independently of GluN2B-NMDAR expression or phosphorylation status (26). Also, the surface redistribution of both GluN2A and GluN2B subunits 24 h

after E2 exposure may contribute to the maintenance of the synaptic potentiation. Even if different effects of E2 have been reported on GluN2A/GluN2B regulation depending on the animal models, timing and stimulation protocols (21, 43), the present findings are consistent with a two-step model in which E2 exposure first favors LTP induction through an increased GluN2B-NMDAR synaptic retention and signaling, and second E2 contributes to LTP maintenance through the control of a GluN2A/GluN2B ratio in the newly-potentiated synapses that prevents further plasticity (38). At the cellular level, our data identify the surface dynamics of NMDAR as a primary target of E2-mediated signaling in hippocampal neurons. How these effects interplay with the role of the receptor current and intracellular signaling remains to be thoroughly explored. Nevertheless, one can speculate that these effects would implicate some of the non-genomic mechanisms of E2 action, *i.e.* E2 action at or near the plasma membrane on either metabotropic glutamate receptor or G-protein estrogen receptor to transduce second messenger cascades and elicit ERK/CREB, mTOR or JNK signaling (for in depth reviews, see 47, 48).

Our behavioral results indicate that surface NMDAR trafficking in the dorsal CA1 subfield of the hippocampus contributes to experience-dependent changes in integrative properties of hippocampal synapses that sustain certain, but not all forms of NMDAR-dependent associative memory. In dorsal CA1, whether in basal condition or in presence of E2, local surface trafficking of NMDAR is selectively required for long-term retention of temporal association between events separated by a brief interval (20 s, *trace* fear conditioning), but neither for contextual/spatial (fear conditioning/object location task) nor elementary (0 s, *delay* fear conditioning) associative memories.

Present selectivity of the surface trafficking manipulation in dorsal CA1 is in agreement with a functional dissociation among dorsal hippocampal subfields, and preferential implication of the CA1 subfield and local NMDAR in the temporal component of memory function (4; reviewed in 49), while spatial and contextual components would rely more on CA3 and DG (50-53). Indeed, while restricting surface trafficking of NMDAR in dorsal CA1 had a selective impact on temporal fear memory, infusion of GluN1 X-link targeting the whole dorsal hippocampus produces an unselective impairment of acquisition of *trace* fear conditioning and retention of both temporal and contextual associative memories *i.e.* all

components previously shown to rely on hippocampal NMDAR (32, 54-56, 57-60). Furthermore, hippocampal NMDAR signaling was found to sustain E2 enhancement of both *trace* fear conditioning and spatial object recognition (10, 13, 61; reviewed in 62).

However, several lines of evidence suggest that the selective effect of GluN1 X-link infusion into the dorsal CA1 for temporal memory cannot be explained entirely by functional regionalization of the hippocampus. First, we found no impact of the infusion of GluN1 X-link in the CA1-dependent object location task (34) while NMDAR besides their role in temporal memory have also been involved in spatial memory (2, 52). Second, GluN1 X-link infusion into the DG has no effect on contextual discrimination whereas this capability was previously shown to rely on DG NMDAR (63, 64). Hence it appears that restricting NMDAR surface trafficking in a particular subfield of the hippocampus, does not affect all associative memory functions of local NMDAR. The behavioral selectivity of GluN1 X-link effects is indicative of GluN1 X-link specificity, which echoes with previous electrophysiological demonstration that GluN1 X-link does not prevent agonist binding or alter functional properties of NMDAR besides lateral mobility (8). Since GluN1-X link only interferes with NMDAR surface trafficking, our data support the conclusion that, in the CA1 subfield of the hippocampus, NMDAR surface diffusion around the synapse is selectively needed to form long-term associative memories of events occurring with a brief temporal interval.

Then, how can one explain the critical implication of CA1 NMDAR surface trafficking in temporal but not contextual/spatial associative memory? The present selectivity of GluN1 X-link effects suggests that surface redistribution of NMDAR around the synaptic area may sustain the detection of co-occurrence between stimuli separated by a brief temporal interval. Although speculative, this proposal is based on the traditional view of NMDAR function according to which these receptors act as detectors of coincident synaptic activations leading to synaptic strengthening that sustain the associative memory of coincident events. In the specific case of temporally discontinuous stimuli (*i.e.* in *trace* fear conditioning), the detection of tone and shock co-occurrence implies that some of synaptic activation induced by the former (tone) persists until the second (shock) occurs (*i.e.* during the *trace* interval). We

suggest that surface NMDAR mobility and its modulation by E2 may contribute to maintain persistent synaptic activation across brief temporal intervals.

In conclusion, our study provides evidence that CA1 NMDAR surface trafficking and its modulation by the sex hormone 17β-estradiol, is a cellular mechanism critical for a major component of episodic memory. As this memory is essential to a normal life and is highly susceptible to degradation in aging and various neuropsychiatric disorders, identifying underlying mechanisms is crucial and the present discovery may have important outcome regarding therapeutic development.

Acknowledgements

ACKNOWLEDGMENTS

This work was supported by l'Institut National de la Santé et de la Recherche Médicale (INSERM), le Centre National de la Recherche Scientifique (CNRS), le Conseil Régional d'Aquitaine, Bordeaux Sciences Agro and le Ministère de l'Enseignement Supérieur et de la Recherche. We thank members of Neurocentre Magendie for constructive discussions.

Financial disclosures

COMPETING FINANCIAL INTERESTS

The authors declare no competing financial interests.

References

REFERENCES

1. Eichenbaum H (2004): Hippocampus: cognitive processes and neural representations that underlie declarative memory. *Neuron*. 44:109-120.

2. Tsien JZ, Huerta PT, Tonegawa S (1996): The essential role of hippocampal CA1 NMDA receptor-dependent synaptic plasticity in spatial memory. *Cell*. 87:1327-1338.

3. Collingridge GL, Isaac JT, Wang YT (2004): Receptor trafficking and synaptic plasticity. *Nat Rev Neurosci*. 5:952-962.

4. Huerta PT, Sun LD, Wilson MA, Tonegawa S (2000): Formation of temporal memory requires NMDA receptors within CA1 pyramidal neurons. *Neuron*. 25:473-480.

5. Taylor AM, Bus T, Sprengel R, Seeburg PH, Rawlins JN, Bannerman DM (2014): Hippocampal NMDA receptors are important for behavioural inhibition but not for encoding associative spatial memories. *Philos Trans R Soc Lond B Biol Sci*. 369:20130149.

6. Tovar KR, Westbrook GL (2002): Mobile NMDA receptors at hippocampal synapses. *Neuron*. 34:255-264.

7. Bard L, Groc L (2011): Glutamate receptor dynamics and protein interaction: lessons from the NMDA receptor. *Mol Cell Neurosci*. 48:298-307.

8. Dupuis JP, Ladepeche L, Seth H, Bard L, Varela J, Mikasova L, et al. (2014): Surface dynamics of GluN2B-NMDA receptors controls plasticity of maturing glutamate synapses. *Embo J*. 33:842-861.

9. McEwen BS (2010): Stress, sex, and neural adaptation to a changing environment: mechanisms of neuronal remodeling. *Ann N Y Acad Sci*. 1204 Suppl:E38-59.

10. Shors TJ, Lewczyk C, Pacynski M, Mathew PR, Pickett J (1998): Stages of estrous mediate the stress-induced impairment of associative learning in the female rat. *Neuroreport*. 9:419-423.

11. Sandstrom NJ, Williams CL (2001): Memory retention is modulated by acute estradiol and progesterone replacement. *Behav Neurosci*. 115:384-393.

12. Luine VN, Jacome LF, Maclusky NJ (2003): Rapid enhancement of visual and place memory by estrogens in rats. *Endocrinology*. 144:2836-2844.

13. Leuner B, Mendolia-Loffredo S, Shors TJ (2004): High levels of estrogen enhance associative memory formation in ovariectomized females. *Psychoneuroendocrinology*. 29:883-890.

14. Hojo Y, Murakami G, Mukai H, Higo S, Hatanaka Y, Ogiue-Ikeda M, et al. (2008): Estrogen synthesis in the brain--role in synaptic plasticity and memory. *Mol Cell Endocrinol*. 290:31-43.

15. Mitra SW, Hoskin E, Yudkovitz J, Pear L, Wilkinson HA, Hayashi S, et al. (2003): Immunolocalization of estrogen receptor beta in the mouse brain: comparison with estrogen receptor alpha. *Endocrinology*. 144:2055-2067.

16. Mitterling KL, Spencer JL, Dziedzic N, Shenoy S, McCarthy K, Waters EM, et al. (2010): Cellular and subcellular localization of estrogen and progestin receptor immunoreactivities in the mouse hippocampus. *J Comp Neurol*. 518:2729-2743.

17. Good M, Day M, Muir JL (1999): Cyclical changes in endogenous levels of oestrogen modulate the induction of LTD and LTP in the hippocampal CA1 region. *Eur J Neurosci*. 11:4476-4480.

18. Gould E, Woolley CS, Frankfurt M, McEwen BS (1990): Gonadal steroids regulate dendritic spine density in hippocampal pyramidal cells in adulthood. *J Neurosci*. 10:1286-1291.

19. Mukai H, Tsurugizawa T, Murakami G, Kominami S, Ishii H, Ogiue-Ikeda M, et al. (2007): Rapid modulation of long-term depression and spinogenesis via synaptic estrogen receptors in hippocampal principal neurons. *J Neurochem*. 100:950-967.

20. Woolley CS, McEwen BS (1992): Estradiol mediates fluctuation in hippocampal synapse density during the estrous cycle in the adult rat. *J Neurosci*. 12:2549-2554.

21. Zamani MR, Desmond NL, Levy WB (2000): Estradiol modulates long-term synaptic depression in female rat hippocampus. *J Neurophysiol*. 84:1800-1808.

22. Woolley CS, Gould E, Frankfurt M, McEwen BS (1990): Naturally occurring fluctuation in dendritic spine density on adult hippocampal pyramidal neurons. *J Neurosci*. 10:4035-4039.

23. Gazzaley AH, Weiland NG, McEwen BS, Morrison JH (1996): Differential regulation of NMDAR1 mRNA and protein by estradiol in the rat hippocampus. *J Neurosci*. 16:6830-6838.

24. Woolley CS, Weiland NG, McEwen BS, Schwartzkroin PA (1997): Estradiol increases the sensitivity of hippocampal CA1 pyramidal cells to NMDA receptor-mediated synaptic input: correlation with dendritic spine density. *J Neurosci*. 17:1848-1859.

25. Smith CC, McMahon LL (2006): Estradiol-induced increase in the magnitude of long-term potentiation is prevented by blocking NR2B-containing receptors. *J Neurosci*. 26:8517-8522.

26. Snyder MA, Cooke BM, Woolley CS (2011): Estradiol potentiation of NR2B-dependent EPSCs is not due to changes in NR2B protein expression or phosphorylation. *Hippocampus*. 21:398-408. .

27. Adams MM, Fink SE, Janssen WG, Shah RA, Morrison JH (2004): Estrogen modulates synaptic N-methyl-D-aspartate receptor subunit distribution in the aged hippocampus. *J Comp Neurol*. 474:419-426.

28. Groc L, Choquet D, Chaouloff F (2008): The stress hormone corticosterone conditions AMPAR surface trafficking and synaptic potentiation. *Nat Neurosci*. 11:868-870.

29. Heine M, Groc L, Frischknecht R, Beique JC, Lounis B, Rumbaugh G, et al. (2008): Surface mobility of postsynaptic AMPARs tunes synaptic transmission. *Science*. 320:201-205.

30. Mingaud F, Le Moine C, Etchamendy N, Mormede C, Jaffard R, Marighetto A (2007): The hippocampus plays a critical role at encoding discontiguous events for subsequent declarative memory expression in mice. *Hippocampus*. 17:264-270.

31. Kaouane N, Porte Y, Vallee M, Brayda-Bruno L, Mons N, Calandreau L, et al. (2012): Glucocorticoids can induce PTSD-like memory impairments in mice. *Science*. 335:1510-1513.

32. Misane I, Tovote P, Meyer M, Spiess J, Ogren SO, Stiedl O (2005): Time-dependent involvement of the dorsal hippocampus in trace fear conditioning in mice. *Hippocampus*. 15:418-426.

33. Fanselow MS (1980): Conditioned and unconditional components of post-shock freezing. *Pavlov J Biol Sci*. 15:177-182.

34. Assini FL, Duzzioni M, Takahashi RN (2009): Object location memory in mice: pharmacological validation and further evidence of hippocampal CA1 participation. *Behav Brain Res*. 204:206-211.

35. Waters EM, Mitterling K, Spencer JL, Mazid S, McEwen BS, Milner TA (2009): Estrogen receptor alpha and beta specific agonists regulate expression of synaptic proteins in rat hippocampus. *Brain Res*. 1290:1-11.

36. Jelks KB, Wylie R, Floyd CL, McAllister AK, Wise P (2007): Estradiol targets synaptic proteins to induce glutamatergic synapse formation in cultured hippocampal neurons: critical role of estrogen receptor-alpha. *J Neurosci*. 27:6903-6913.

37. Murphy DD, Segal M (1996): Regulation of dendritic spine density in cultured rat hippocampal neurons by steroid hormones. *J Neurosci*. 16:4059-4068.

38. Srivastava DP, Woolfrey KM, Jones KA, Shum CY, Lash LL, Swanson GT, et al. (2008): Rapid enhancement of two-step wiring plasticity by estrogen and NMDA receptor activity. *Proc Natl Acad Sci U S A*. 105:14650-14655.

39. Woolley CS, McEwen BS (1994): Estradiol regulates hippocampal dendritic spine density via an N-methyl-D-aspartate receptor-dependent mechanism. *J Neurosci*. 14:7680-7687.

40. Barker GR, Warburton EC (2011): When is the hippocampus involved in recognition memory? *J Neurosci*. 31:10721-10731.

41. Nabavi S, Kessels HW, Alfonso S, Aow J, Fox R, Malinow R (2013): Metabotropic NMDA receptor function is required for NMDA receptor-dependent long-term depression. *Proc Natl Acad Sci U S A*. 110:4027-4032.

42. Eichenbaum H (2013): Memory on time. *Trends Cogn Sci*. 17:81-88.

43. Woolley CS (2007): Acute effects of estrogen on neuronal physiology. *Annu Rev Pharmacol Toxicol*. 47:657-680.

44. Smith CC, Vedder LC, McMahon LL (2009): Estradiol and the relationship between dendritic spines, NR2B containing NMDA receptors, and the magnitude of long-term potentiation at hippocampal CA3-CA1 synapses. *Psychoneuroendocrinology*. 34 Suppl 1:S130-142.

45. Lau CG, Zukin RS (2007): NMDA receptor trafficking in synaptic plasticity and neuropsychiatric disorders. *Nat Rev Neurosci*. 8:413-426.

46. Yashiro K, Philpot BD (2008): Regulation of NMDA receptor subunit expression and its implications for LTD, LTP, and metaplasticity. *Neuropharmacology*. 55:1081-1094.

47. Frick KM (2015): Molecular mechanisms underlying the memory-enhancing effects of estradiol. *Horm Behav*.

48. Tuscher JJ, Fortress AM, Kim J, Frick KM (2015): Regulation of object recognition and object placement by ovarian sex steroid hormones. *Behav Brain Res*. 285:140-157.

49. Kesner RP, Lee I, Gilbert P (2004): A behavioral assessment of hippocampal function based on a subregional analysis. *Rev Neurosci*. 15:333-351.

50. Hunsaker MR, Tran GT, Kesner RP (2009): A behavioral analysis of the role of CA3 and CA1 subcortical efferents during classical fear conditioning. *Behav Neurosci*. 123:624-630.

51. McHugh TJ, Tonegawa S (2009): CA3 NMDA receptors are required for the rapid formation of a salient contextual representation. *Hippocampus*. 19:1153-1158.

52. Place R, Lykken C, Beer Z, Suh J, McHugh TJ, Tonegawa S, et al. (2012): NMDA signaling in CA1 mediates selectively the spatial component of episodic memory. *Learn Mem*. 19:164-169.

53. Rogers JL, Hunsaker MR, Kesner RP (2006): Effects of ventral and dorsal CA1 subregional lesions on trace fear conditioning. *Neurobiol Learn Mem*. 86:72-81.

54. Bast T, Zhang WN, Feldon J (2003): Dorsal hippocampus and classical fear conditioning to tone and context in rats: effects of local NMDA-receptor blockade and stimulation. *Hippocampus*. 13:657-675.

55. Czerniawski J, Ree F, Chia C, Otto T (2012): Dorsal versus ventral hippocampal contributions to trace and contextual conditioning: differential effects of regionally selective NMDA receptor antagonism on acquisition and expression. *Hippocampus*. 22:1528-1539.

56. Gao C, Gill MB, Tronson NC, Guedea AL, Guzman YF, Huh KH, et al. (2010): Hippocampal NMDA receptor subunits differentially regulate fear memory formation and neuronal signal propagation. *Hippocampus*. 20:1072-1082.

57. Quinn JJ, Loya F, Ma QD, Fanselow MS (2005): Dorsal hippocampus NMDA receptors differentially mediate trace and contextual fear conditioning. *Hippocampus*. 15:665-674.

58. Schenberg EE, Oliveira MG (2008): Effects of pre or posttraining dorsal hippocampus D-AP5 injection on fear conditioning to tone, background, and foreground context. *Hippocampus*. 18:1089-1093.

59. Stiedl O, Birkenfeld K, Palve M, Spiess J (2000): Impairment of conditioned contextual fear of C57BL/6J mice by intracerebral injections of the NMDA receptor antagonist APV. *Behav Brain Res*. 116:157-168.

60. Wanisch K, Tang J, Mederer A, Wotjak CT (2005): Trace fear conditioning depends on NMDA receptor activation and protein synthesis within the dorsal hippocampus of mice. *Behav Brain Res*. 157:63-69.

61. Vedder LC, Smith CC, Flannigan AE, McMahon LL (2013): Estradiol-induced increase in novel object recognition requires hippocampal NR2B-containing NMDA receptors. *Hippocampus*. 23:108-115.

62. Dalla C, Shors TJ (2009): Sex differences in learning processes of classical and operant conditioning. *Physiol Behav*. 97:229-238.

63. Eadie BD, Cushman J, Kannangara TS, Fanselow MS, Christie BR (2012): NMDA receptor hypofunction in the dentate gyrus and impaired context discrimination in adult Fmr1 knockout mice. *Hippocampus*. 22:241-254.

64. Kheirbek MA, Tannenholz L, Hen R (2012): NR2B-dependent plasticity of adult-born granule cells is necessary for context discrimination. *J Neurosci*. 32:8696-8702.

Footnotes

Table/Figure legends

FIGURE LEGENDS

Figure 1. E2 increases synaptic density, surface GluA1-AMPAR content and regulates surface distribution of GluN2-NMDAR. (A) E2 treatment increases the postsynaptic density (PSD) and the surface GluA1-AMPAR content. *Top panel:* Dendritic segment of a Homer 1c-DS-Red expressing hippocampal neuron treated with vehicle or E2 (10 nM, 24h). Scale bar=2 μm. *Bottom panel:* Surface GluA1-AMPAR were immunolabelled after vehicle (open bars) and E2 (black bars) treatment. Note the increase in surface staining intensity (color-coded: low value in blue and high value in red-white). Scale bar=300nm. **(B)** Comparison of the synaptic density and synaptic size (*top*), synaptic and total surface GluA1-AMPAR content (*bottom*) after vehicle (open bars) and E2 (black bars) treatment. Data are derived from at least 3 independent experiments. Histograms show mean±sem of percent of vehicle (for synaptic density: N=47/41; t_{86}=7.212; p<0.0001; for synaptic size N=18/17; t_{33}=0.1513; p=0.4403; for synaptic GluA1 N=8/10; t_{16}=2.393; p=0.0147 and for total GluA1 N=14/14; t_{26}=2.506; p=0.0094, for vehicle/E2-treated hippocampal neurons, respectively). **(C)** Immunocytochemical detections of endogenous surface GluN2A- and GluN2B-NMDAR in vehicle and E2-treated hippocampal neurons. PSD were identified by Shank staining. Some surface GluN2 staining co localize with Shank staining (overlay in yellow). Scale bar=2 μm. **(D)** Comparisons of the synaptic content of surface GluN2A- and GluN2B-NMDAR between vehicle (open bars) and E2 (black bars) conditions. Histograms show mean±sem of percent of vehicle (GluN2A-NMDAR: N=14/14; t_{26}=2.813; p=0.0046 and GluN2B-NMDAR: N=37/37, t_{72}=2.847; p=0.0029 for vehicle/E2-treated neurons, respectively). Student's *t*-tests were performed for comparisons between vehicle- and E2-treated hippocampal neurons. *, ** and *** indicate p<0.05, 0.01 and 0.001, respectively.

Figure 2. E2 regulates surface diffusion of GluN2-NMDAR and reduction of NMDAR surface diffusion impairs E2-induced increase in dendritic spine density *in vitro*. (A) Schematic representation of the QD single nanoparticle tracking approach. **(B)** E2 acutely regulates the surface diffusion of GluN2B-NMDAR.

Representative trajectories of surface GluN2B-NMDAR-QD before (basal) and after E2 treatment (10 nM, 15min). The grey areas correspond to synaptic sites labeled with Mitotracker. Scale bar=100nm. **(C)** Comparisons of the instantaneous diffusion coefficient (left panel) and of synaptic dwell-time (right panel) of synaptic GluN2A and GluN2B-NMDAR (n=6-7 dendritic fields; 23-26 trajectories/group; respectively) before and after E2 treatment (diffusion coefficient: p=0.102 and p=0.041; dwell time: p=0.21 and p=0.0140 for GluN2A- and GluN2B-NMDAR, respectively). **(D)** Representative trajectories of surface GluN2A- and/or GluN2B-NMDAR in hippocampal neurons treated with vehicle solution or E2 (scale bar=200 nm). In vehicle condition, GluN2A-NMDAR are less mobile and more synaptic than GluN2B-NMDAR. E2 treatment (10 nM, 24h) favors the synaptic anchoring of GluN2A-NMDAR and lateral escape of GluN2B-NMDAR to extrasynaptic areas. **(E)** Cumulative distribution of the instantaneous diffusion coefficient of GluN2A- and GluN2B-NMDAR in the synaptic area of vehicle (GluN2A-NMDAR: 127; GluN2B-NMDAR: 153 trajectories) and E2-treated neurons (GluN2A-NMDAR: 117; GluN2B-NMDAR: 237 trajectories). **(F)** Relative comparisons of the instantaneous diffusion coefficient of GluN2A- and GluN2B-NMDAR in synapses between vehicle and E2 conditions (p=0.0029 and 0.0051 for GluN2A- and GluN2B-NMDAR respectively) **(G)** Schematic representation of the GluN1 NMDAR X-link procedure. **(H)** Shank clusters fluorescently-detected in dendritic fields of hippocampal neurons following vehicle-, E2 (10 nM) with GluN2A X-link or GluN2B X-link treatments. Scale bar=5 µm. (**I**) Comparison of the Shank cluster density in the different conditions (vehicle/E2, n=124/131; GluN2A-NMDAR: n=22/21; GluN2B-NMDAR: n=53/44 dendritic fields, respectively; one way ANOVA: $F_{5,389}$=32.3; p<0.0001). Error bars represent sem. *, ** and *** indicate p<0.05, p<0.01 and p<0.001 respectively (Non-parametric Mann-Whitney test, Student *t*-test and One way ANOVA followed by Bonferroni *post-hoc* comparisons where applicable).

Figure 3. Surface cross-linking of GluN1-NMDAR impairs electrically and E2-induced NMDAR-dependent LTP *in vivo* in adult mice. (A) Experimental design of electrophysiological *in vivo* recording of

CA1 fEPSP in anesthetized mice. CA3 fibers from the contralateral hippocampus were stimulated (STIM) and field potentials were recorded (REC) in CA1 before and after high frequency stimulation (HFS, 100 Hz, 1s). **(B)** Representative histological controls of REC and STIM sites. **(C)** Representative fEPSP traces before (1) and after (2) CNQX application. **(D)** NMDAR antagonists (AP5, 100 μM, 60 nL intra-CA1 5 min pre-HFS; MK801, 3 mg/kg, *ip* 45 min pre-HFS) blocked the HFS-induced LTP (*Treatment*: $F_{2,10}$=8.8; p=0.006). **(E)** Representative fEPSP traces before (1) and after (2) GluN1 X-link infusion. Neither control nor GluN1 X-link infusions change basal synaptic transmission at least for 40 min after infusions (*Time*: $F_{9,50}$=2.7; p=0.0128; *Treatment:* $F_{1,50}$=2.8; p=0.0994 and *Treatment x Time*: $F_{9,50}$=0.4; p=0.9426). GluN1 X-link impairs HFS-induced LTP **(F)** and E2-induced LTP **(G)**. Representative fEPSP traces before (1) and after (2) HFS/E2 after control (open circles) or GluN1 X-link (filled circles) infusions and corresponding plots (*Time*: $F_{9,110}$=3.2; p=0.0018; *Treatment:* $F_{1,110}$=82.0; p<0.0001; *Treatment x Time*: $F_{9,110}$=3.3, p=0.0013 **(F)** and *Time*: $F_{9,110}$=3.8; p=0.0003; *Treatment:* $F_{1,110}$=20.3; p<0.0001; *Treatment x Time*: $F_{9,110}$=2.3; p=0.0212 **(G)**. All graphs show mean±sem of change from baseline. Sample sizes (number of animals) are indicated in legends/within bars. *, ** and *** indicate p<0.05, p<0.01 and p<0.001 respectively (one or two-way ANOVA followed by Bonferroni *post-hoc* comparisons, where applicable).

Figure 4. Reduction of NMDAR surface dynamics in the dorsal hippocampus (CA1) selectively impairs temporal associative memory. (A) Schematic representation of the experimental procedure. Bilateral intra-CA1 infusions (GluN1 X-link/control, 300 nL per side) were performed 45 min before *trace* fear conditioning (five pairings of tone (65 dB, 1 kHz, 30 s) and foot shock (0.6 mA, 50 Hz, 1 s) with a 20 s interval. Retention of temporal and contextual fear memories, respectively based on a 20 s *trace* tone-shock association and a context-shock association, were measured during re-exposure to the tone alone in a neutral context (context B, tone, 24 h after conditioning) and to the conditioning context (context A, context, 2 h after tone test). Graphs show the percentage of time spent freezing **(C)** during the tone relative to the no tone periods (*i.e.*, pre- and post-tone in context B and **(D)** during re-exposure to conditioning context (A) relative to the neutral context (B). **(B)** Representative photography showing

location of intra-CA1 *cannulae* and the extent of GluN1 X-link diffusion 45 min after infusion in living mice and revealed with only secondary antibody (Scale bar=250µm). **(C) Conditioning:** GluN1 X-link spares the acquisition of *trace* fear conditioning. The increase of time spent freezing over repeated tone presentations is not different between groups (*Tone repetition*: $F_{4,64}$=25.2; p<0.0001; *Treatment* $F_{1,16}$=0.5; p=0.5063 and *Interaction*: $F_{4,64}$=0.5; p=0.7114). **(D-E) Retention:** GluN1 X-link diminishes the 24h retention of fear memory based on a temporal association (**D, Tone:** *Tone*: $F_{1,32}$=23.0; p<0.0001; *Treatment:* $F_{1,32}$=2.2; p=0.1496; *Interaction*: $F_{1,32}$=4.7; p=0.0381) but not contextual association (**E, Context:** *Context*: $F_{1,32}$=43.7; p<0.0001; *Treatment*: $F_{1,32}$=1.0; p=0.3178 and *Interaction*: $F_{1,32}$=1.1; p=0.3043). All graphs show mean±sem of percent of time spent freezing (% freezing); n=numbers of animals. Statistical comparisons to control condition or within experimental groups are indicated by * and *** for p<0.05 and p<0.001, respectively (two-way ANOVA and Bonferroni *post-hoc comparisons*).

Figure 5: Reduction of NMDAR surface dynamics in the dorsal hippocampus (CA1) does not impairs object location memory. (A) Schematic representation of the experimental procedure. Bilateral intra-CA1 infusions (GluN1 X-link/control, 300 nL per side) were performed 45 min before *acquisition* phase (10 minutes of freely behaving in an open field containing 2 identical objects). Retention of object location was measured during the *test* phase 24h after *acquisition*. *Test* Phase consists in re-exposure to the open field in which one of the objects (A') was moved to a new location (displaced object = DO). Graphs show the location index, defined as the *ratio* between the time (T) spent exploring DO (A') and non-displaced object (NDO, A) over the time spent exploring both objects [$T_{DO}/(T_{DO}+T_{NDO})$] and [$T_{NDO}/(T_{DO}+T_{NDO})$] during the *acquisition* phase **(C)** and during the *test* phase **(D).** GluN1 X-link spares the acquisition of *object location memory* and the 24 h retention of this memory. Indeed, whichever the treatment condition, in the *acquisition* phase the location index is neither different from chance (0.5, dashed line) nor different between objects (**B,** *Object*: $F_{1,21}$=0.0; p=0.9829; *Treatment* $F_{1,21}$=4,2; p=0.0531 and *Interaction*: $F_{1,21}$=0.25 p=0.6222). In the *Test* phase, location indexes are different from chance (0.5 dashed line) and between objects for both treatment groups and with no difference between the 2

groups (**C,** *Object*: $F_{1,21}$=13.18; p=0.00016; *Treatment:* $F_{1,21}$=1.1 p=0.3071 *Interaction*: $F_{1,21}$=0.21; p=0.6486). All graphs show mean±sem of location index; n=numbers of animals. Statistical comparisons to control condition or within experimental groups are indicated by * and *** for p<0.05 and p<0.001, respectively (two-way ANOVA and student's t tests *post-hoc* comparisons).

Figure 6. Reduction of surface NMDAR surface dynamics in the dorsal (CA1) hippocampus selectively impairs E2 enhancement of temporal associative memory. Bilateral intra-CA1 E2 infusions prior to conditioning (0,3 mA shock intensity) enhances the 24 h retention of tone shock association in both *trace* (20 s, **A**) and *delay* (0 s, **B**) fear conditioning and GluN1 X-link prevents the E2-induced enhancement of associative memory only in *trace* conditioning. **(A) Tone (*trace*, 20 s)**: Overall interaction: $F_{3,40}$=7.45 p=0.0004; treatment effect: $F_{3,40}$=1.9; p=0.1410; tone effect: $F_{1,40}$=23.7; p<0.0001; **Control:** *E2 treatment x Tone* $F_{1,21}$=4.9; p=0.00373; **GluN1 X-link***: E2 treatment* and *Interaction p>0.05*; **E2:** *GluN1 X-link treatment x Tone* $F_{1,17}$=5.9; p=0.0264) but not in *delay* (0s) conditioning. **(B): Tone (*delay*, 0 s):** Overall interaction: $F_{3,44}$=3.3; p=0.0287; Treatment effect: $F_{3,44}$=3.5; p=0.0233; Tone effect: $F_{1,44}$=52.8; p<0,0001; **E2***, GluN1 X-link treatment x Tone*: p>0.05; **GluN1 X-link***, E2 treatment x Tone:* $F_{1,23}$=5.21; p=0.0321). **(C-D)** There is no effect on context retention whatever the conditioning condition and all groups exhibit higher freezing levels in the conditioning context (A)- than the neutral one (B). Overall interaction: $F_{3,40}$=1.8 p=0.1608 and $F_{3,44}$=1.6 p=0.2006; Treatment effect: $F_{3,40}$=1.9; p=0.1479 and $F_{3,44}$=1.35; p=0.2703; Context effect: $F_{1,40}$=71.4; p<0.0001 and $F_{1,44}$=39.4; p<0.0001, for *trace* **(C)** and *delay* **(D)** condition, respectively). All histograms show mean±sem; n=number of animals. Comparisons *vs.* no-tone **(A-B)** or neutral context **(C-D)** are indicated by *, ** and *** for p<0.05, p<0.01 and p<0.001, respectively (two-way ANOVA followed by *post-hoc* student's t tests).

Figure 1

Potier et al.

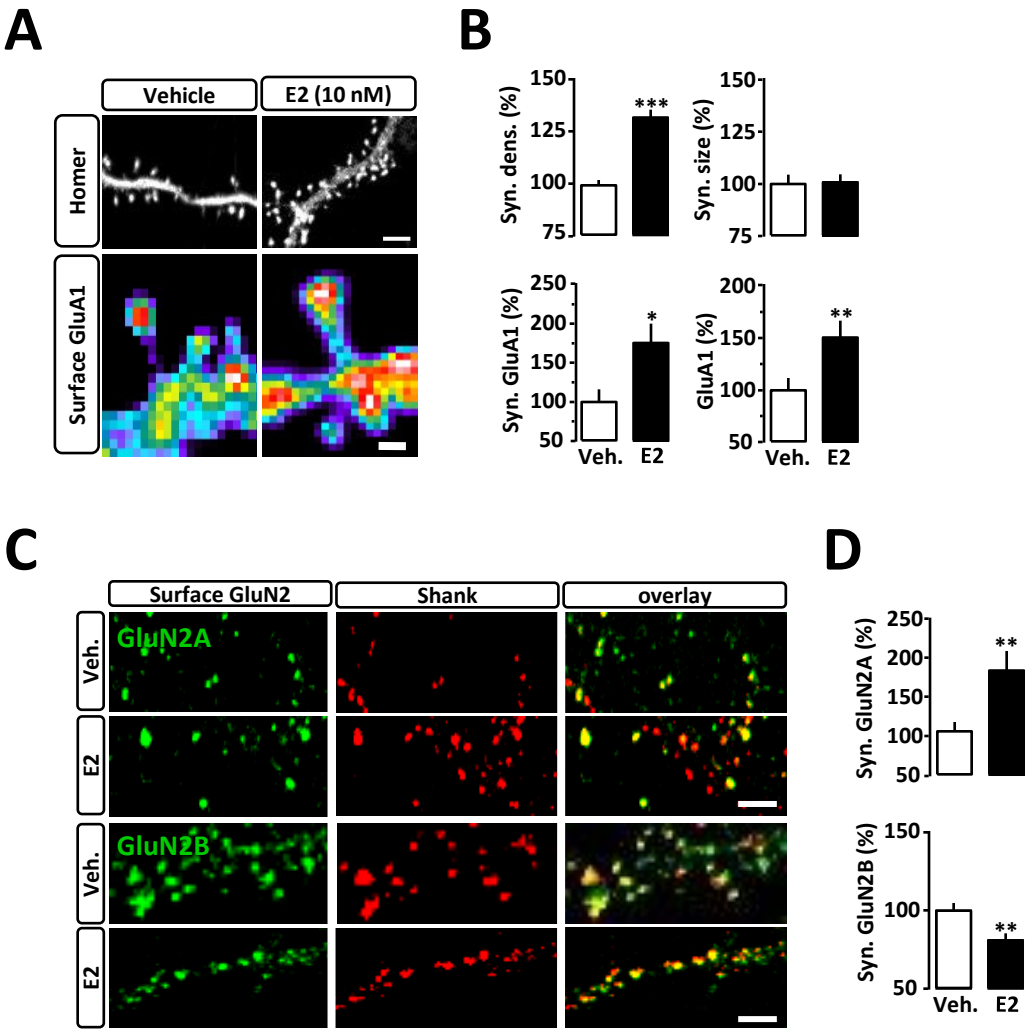

Figure 2

Potier et al.

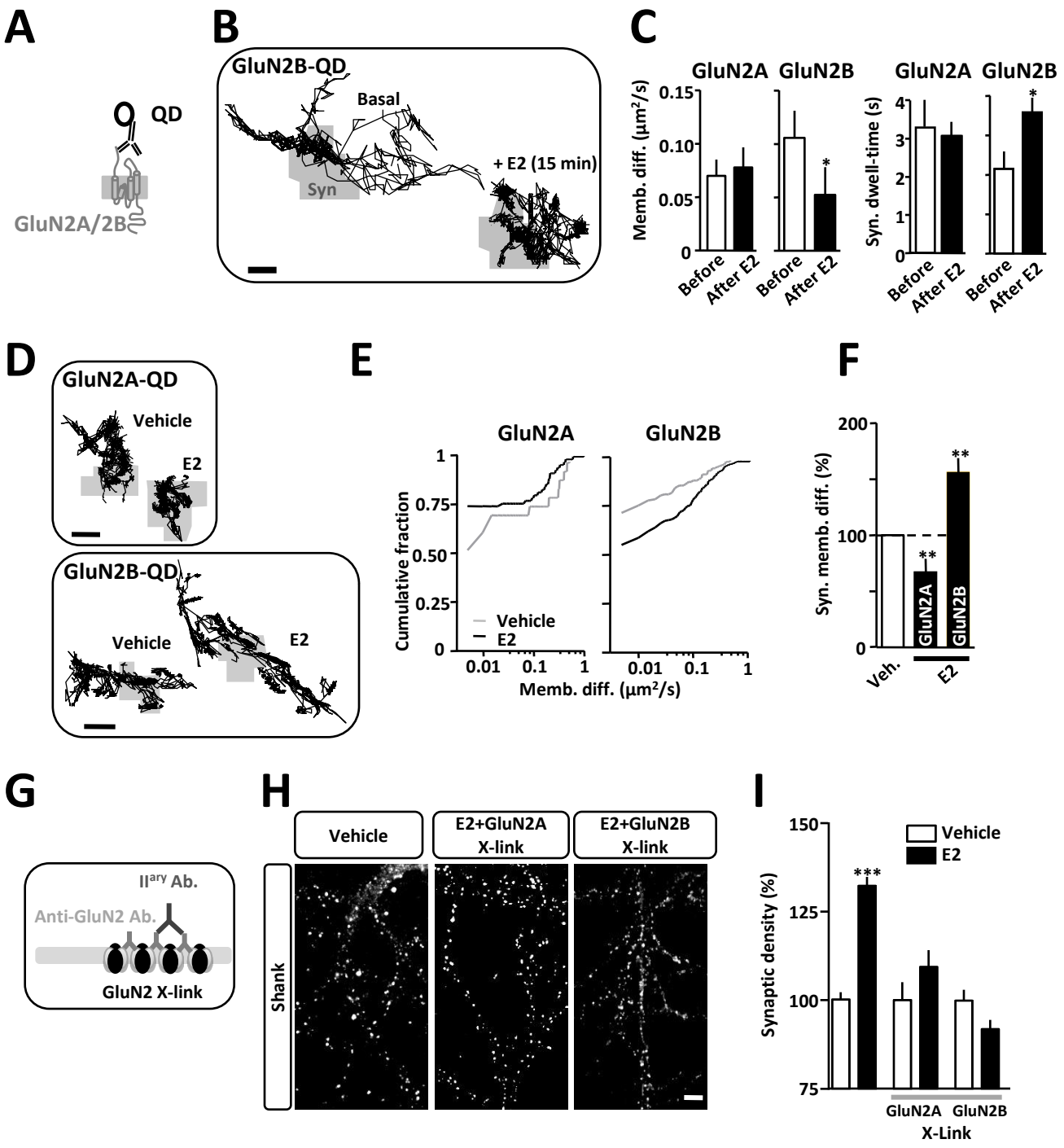

Figure 3

Potier et al.

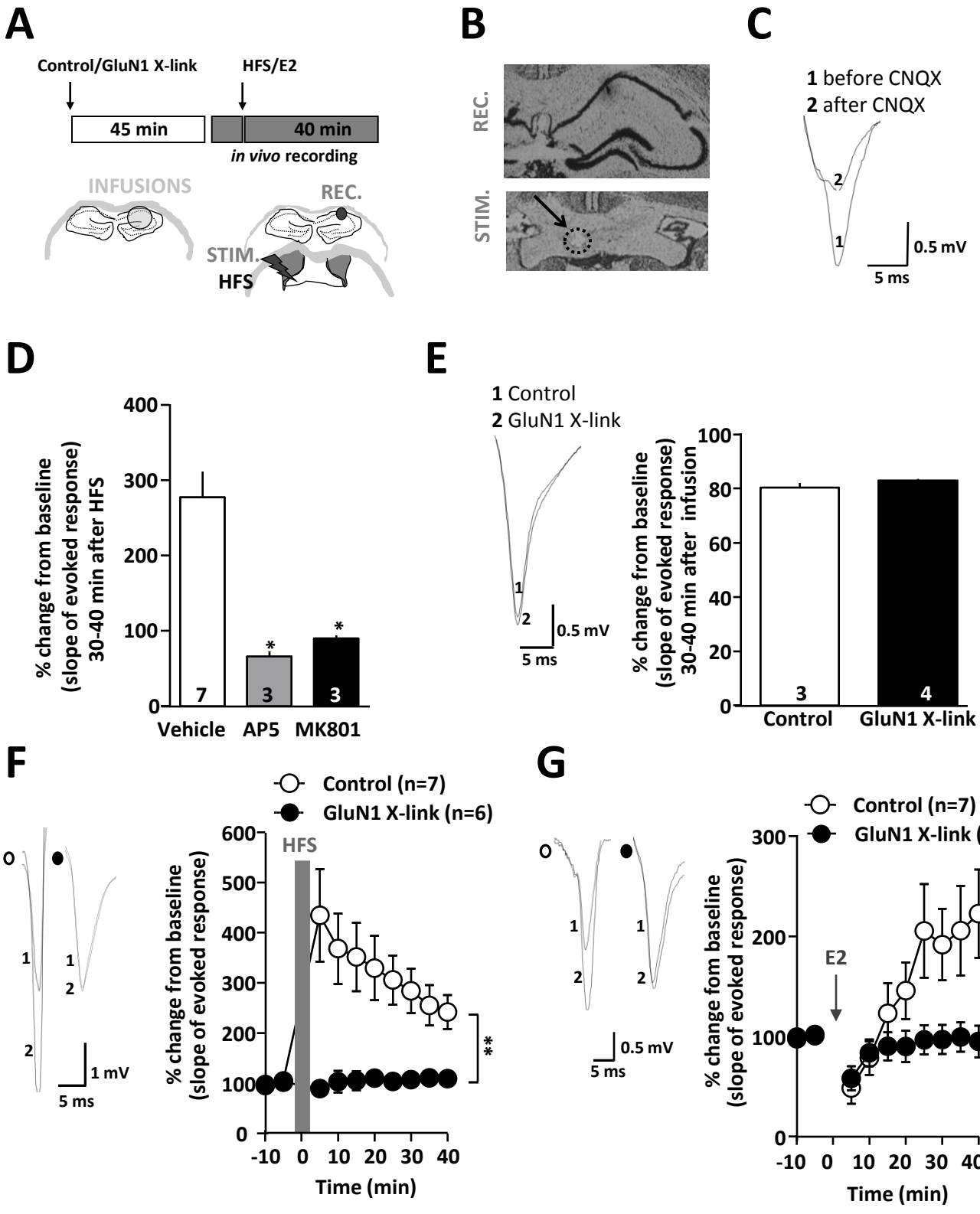

Figure 4

Potier et al.

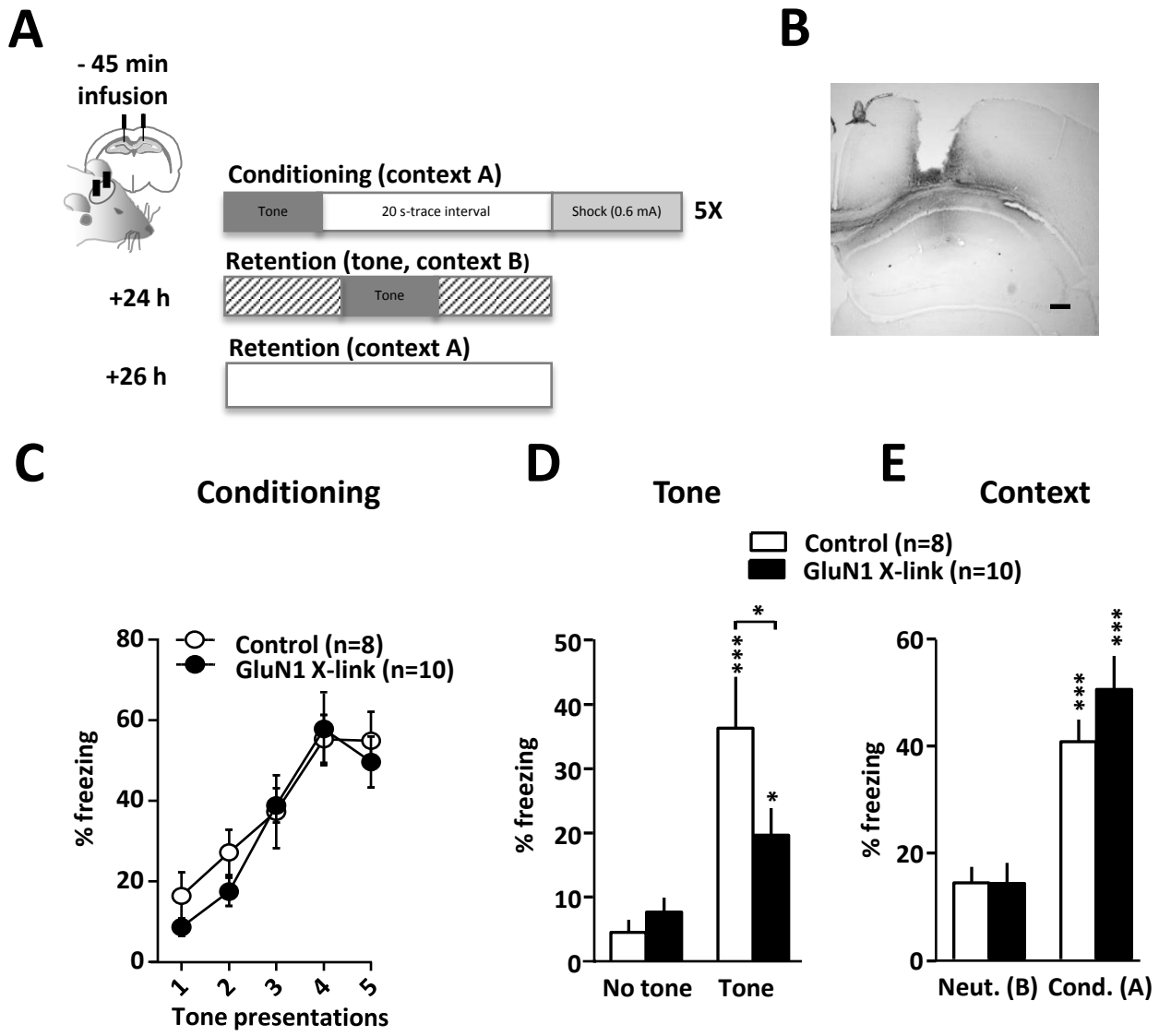

Figure 5

Potier et al.

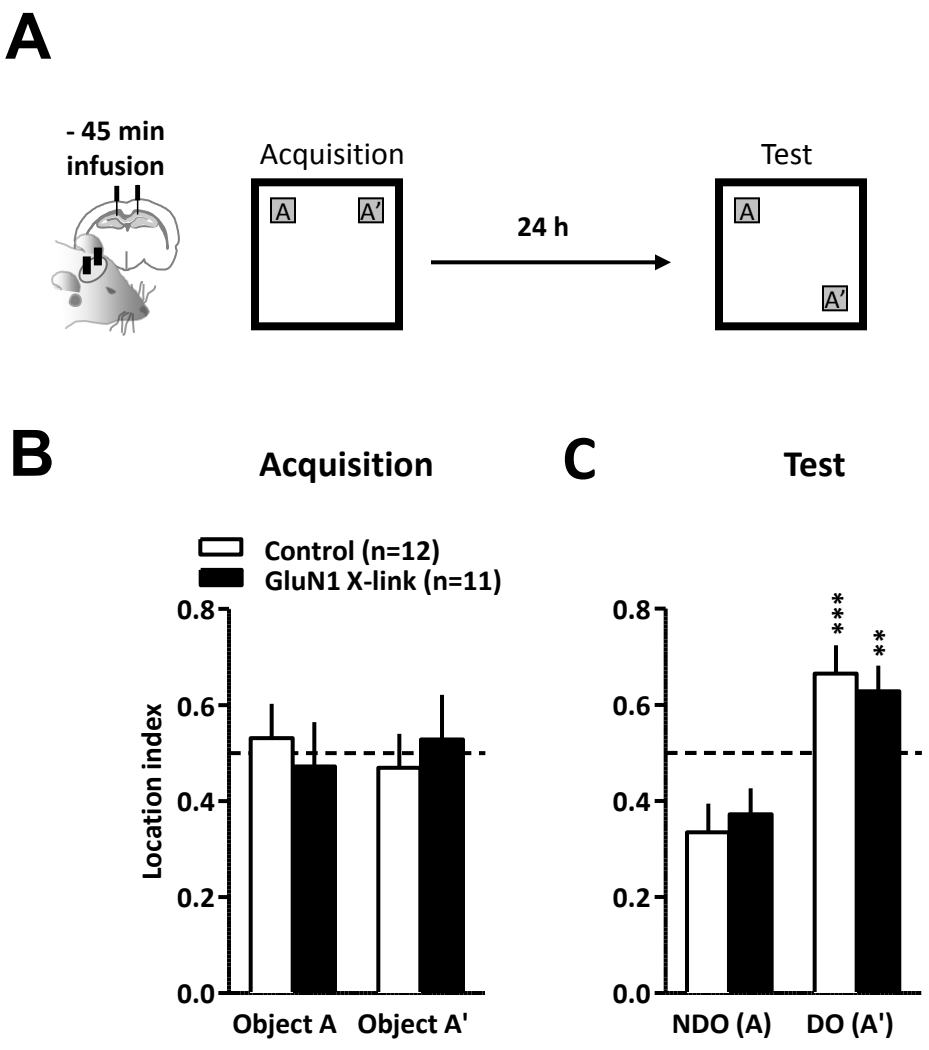

Figure 6

Potier et al.

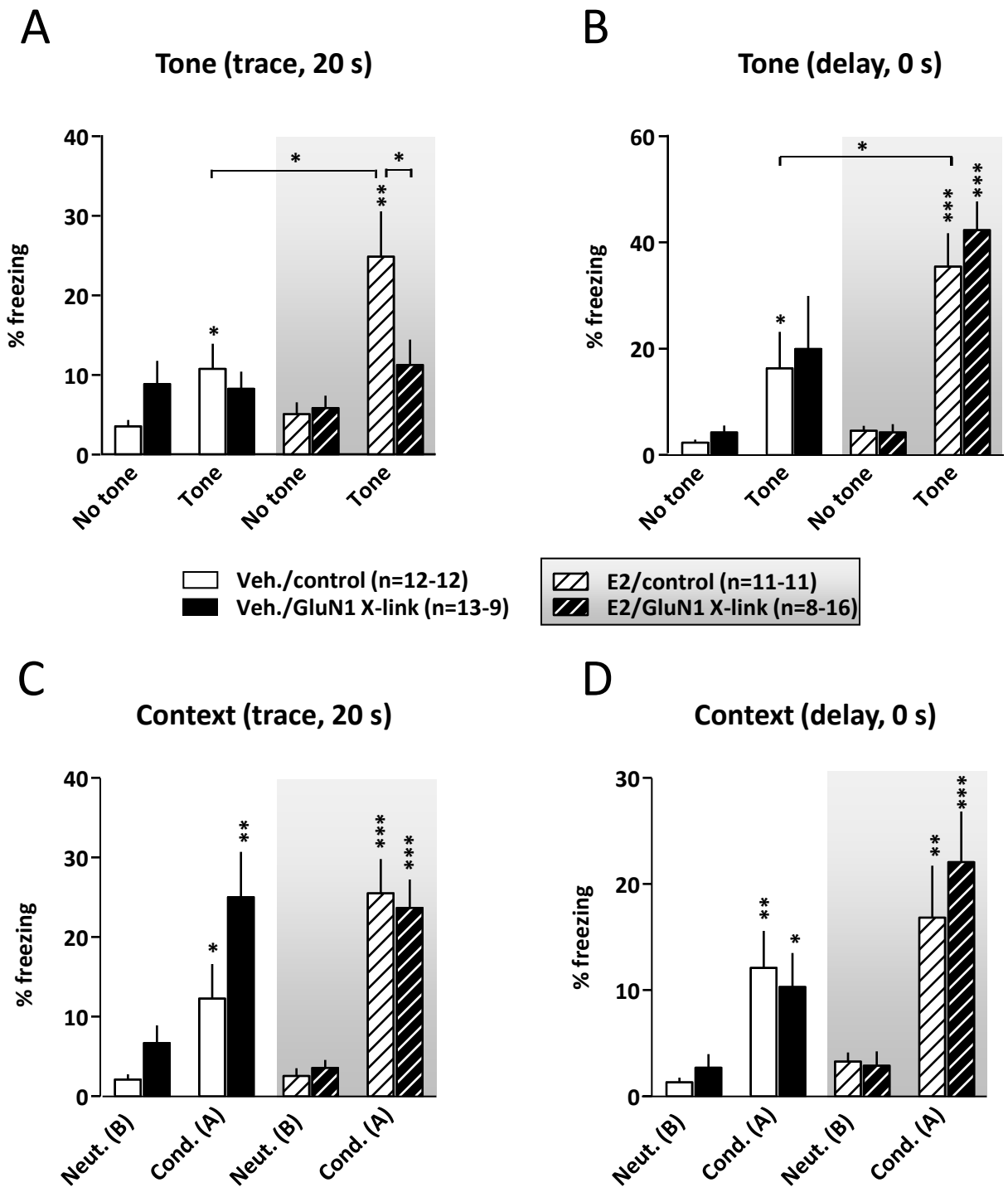

Potier et al

Temporal memory and its enhancement by estradiol requires surface dynamics of hippocampal CA1 NMDA receptors

Supplemental Information

Supplemental Material and Methods

Cell culture, protein expression, synaptic live staining and immunocytochemistry

Hippocampal neurons from 18 days-old rat embryos were cultured on glass coverslips following the Banker technique as previously described (1-3). Cells were plated at a density of $200x10^3$ cells per mL on poly-lysine pre-coated cover slips and cultures were maintained in serum-free neurobasal medium (Invitrogen, France) at 37°C, 5% CO2 for up to 22 days *in vitro* (div). For some experiments, neurons were transfected at 9-10 div with Homer1c-DsRed and SEP-GluA1 using the Effectene transfection kit (Qiagen, France) according to manufacturer's instructions.

Surface GluN2A and GluN2B subunits containing NMDAR staining was performed for 10 min on live neurons at 37°C in culture medium using antibodies directed against epitopes corresponding to residues 41-53 and 323-327 of GluN2A and GluN2B subunits, respectively (Alomone Labs, Israel). Surface GluA1 staining was performed on neurons previously transfected with SEP-GluA1 and immunolabeled using a mouse monoclonal anti-GFP antibody (1/400; Roche). Neurons were then fixed, washed and finally incubated 30 min with secondary antibody anti-mouse Alexa Fluor 488 (1/800, Molecular Probes, France). To label postsynaptic areas, neurons were permeabilized using 0.1% Triton X100, incubated 30 min with a primary rabbit polyclonal directed against Shank (1/1000, Abcam, France) or mouse monoclonal PSD-95 antibodies (1/800, Neuromab, France) and incubated with secondary antibody anti-rabbit or anti mouse Alexa 568 (1/1000, 30 min, Molecular Probes, France). Neurons were washed, mounted and preparations were kept at 4°C until image acquisition

and analysis. Immunolabeled or over-expressed fluorescent proteins were imaged using a spinning confocal microscope (Leica, Germany) with a 63x oil immersion objective.

For each experiment, 2-6 different sets of hippocampal cultures were used. For each condition, 8-12 neurons (N, from at least 3 separate experiments) were used and at least 2 dendritic fields (n) from each neuron were analyzed. To quantify spine density, the dendritic length was manually obtained and individual spines were counted over those segments. The quantification of the receptor surface staining, the average intensity and area of fluorescently-labelled surface receptor (total or within synaptic cluster) were measured within dendritic fields using imaging tools from Metamorph software (Universal Imaging Corporation, PA, USA) as previously published (2-4). The integrated fluorescence levels were averaged and expressed as percentage compared to vehicle-treated group.

Single particle (Quantum dot) tracking and surface diffusion

As previously described (5-7), the nanoparticle QD 655 Goat F(ab')$_2$ anti-Rabbit IgG (Invitrogen, France) were first incubated for 30 minutes with polyclonal antibodies directed against GluN2A or GluN2B subunits (same as above). Non-specific binding was blocked by additional casein (Vector Laboratories, France). Neurons were then incubated for 10 min with pre-coated anti-rabbit QD (1:10000) and mounted on a heated-chamber for observation. QD signals were detected using an EMCCD camera (Quantem, Roper Scientific, Germany) and followed on randomly selected dendritic regions for up to 20 min. QD recording sessions were processed with the Metamorph software. The instantaneous diffusion coefficient 'D' was calculated for each trajectory, from linear fits of the first 4 points of the mean-square-displacement versus time function using MSD(t)=<r2> (t)=4Dt. The two-dimensional trajectories of single molecules in the plane of focus were constructed by correlation analysis between consecutive images using a Vogel algorithm.

Drug treatments and cross-link (X-Link) procedure *in vitro*

Neurons were treated with 10 nM of E2 (17β-estradiol, Sigma, France) or vehicle solution (0.0001% DMSO, Sigma, France) in culture medium (for 15 min or 24 h, as indicated) before processing neurons

for immunostaining or single particle tracking. To affect the surface diffusion of GluN2-containing NMDAR, we used, prior to E2 treatment, the X-link procedure (figure 2G) adapted from previous published studies (6, 7). This procedure was shown to alter synaptic plasticity without altering intrinsic capability of NMDAR to respond to glutamate(5). Schematically, neurons were incubated with highly concentrated (0.2 mg/mL) polyclonal antibodies directed against GluN2A or GluN2B or goat anti-rabbit IgG antibody (0.2 mg/mL; control, Invitrogen, France) for 30 min before E2 or vehicle addition into culture medium.

Animals

For *in vivo* studies, we used 3-4 month-old naive male mice (C57Bl/6J; Janvier, France) collectively (8 mice/cage) housed in standardized animal room conditions (22±1°C, 65% humidity, light on: 07:00-19:00) with *ad libitum* access to food and water. All experiments took place during the light phase. Before electrophysiological and behavioral experiments, animals were randomly selected from collective cages and assigned to experimental groups. For behavioral experiments, the mice were shifted to individual housing from before surgery to the end of experiments. The number of mice by group was determined on basis of previous studies using the same procedures (8, 9). All animal care and behavioral tests were conducted in compliance with the European Communities Council Directive 2010-63-EU and approved by the *Bordeaux University Animal care and use committee* under the protocol number 5012070-A.

***In vivo* electrophysiology in anesthetized mice**

Field excitatory postsynaptic potentials (fEPSP) evoked by stimulation of CA3 input in CA1 synapses were recorded. Briefly, stereotaxic surgery for electrophysiology experiments was performed under isoflurane *anaesthesia* (1.0-1.2%, O_2 flow rate: 1L/min) as described previously (8). Mice's body temperature was maintained using at 37°C using a temperature control system (FHC, ME, USA). Concentric bipolar stimulating electrodes (Rhodes Medical Instruments, CA, USA) were inserted into the ventral hippocampal commissure (anteroposterior: -0.5 mm from *bregma*, mediolateral: +0.3

mm from midline on the left hemisphere; dorsoventral: 2.3 mm from brain surface) as described previously (10).

GluN1 NMDAR surface mobility was blocked using the X-link protocol against GluN1 subunit to immobilize surface NMDAR (5) (epitope corresponding to residues 385-399 of GluN1 subunit; Alomone Labs, Israel). Forty-five minutes before HFS (1 train of 1s at 100 Hz) or CA1 infusion of E2 (10 nM, 60 nL), GluN1 X-link (0.2 mg/mL) or goat anti-rabbit IgG antibody (control) was infused (figure 3A) into the dorsoventral axis of CA1 area (3 consecutive infusions of 60 nL at 30 s intervals at 1.0, 1.25 and 1.5 mm from brain surface) using controlled pressure-pulses of compressed air (20 psi, 2 min period, 180 nL total volume) applied via a Picospritzer® (Parker Hannifin, NJ, USA) to a single or a double-barrel glass recording micropipette. fEPSP were recorded through a glass recording electrode, filled with 0.5 M sodium acetate/2% pontamine sky blue, inserted in area CA1 *stratum radiatum* (anteroposterior: -1.8 mm from *bregma*, mediolateral: -1.25 mm from midline on the right hemisphere; dorsoventral: 1.2-1.4 mm from brain surface) as previously described (8). In a subset of experiments AP5 (Sigma, France, 100 μM, 60 nL intra-CA1) was infused 5 min before HFS and MK801 (Sigma, France, 3 mg/kg) was injected *ip* 45 min before HFS. fEPSP were amplified (Axoclamp2B amplifier, Molecular devices, CA, USA) and filtered (differential AC amplifier, model 1700; A-M Systems, WA, USA), digitized and collected on-line using a laboratory interface and software (CED 1401, SPIKE 2; Cambridge Electronic Design, UK). Basal stimulation intensity was adjusted to 30-40% of the maximum evoked field response. All responses were expressed as percent change from the average responses recorded during the 10 min before drug application or HFS. At the end of each recording experiment, the electrical stimulation site and the recording electrode placement were marked. Histological controls of stimulation and recording sites were used as exclusion criteria and sample size was based on previous studies using similar experimental procedure (8, 10).

Surgical procedures

Surgery and intra-hippocampal infusions in freely moving mice were performed as described previously (9, 11). Briefly**,** mice were anesthetized with ketamine-xylazine (80-16 mg/kg body weight*,*

ip) and secured in a stereotaxic frame (Kopf Instruments). Stainless-steel guide *cannulae* (26 gauge, 8 mm length) were implanted bilaterally 0.8 mm above the dorsal hippocampus (anteroposterior, -2 mm; mediolateral, +1.3 mm; dorsoventral, 0.8 mm; relative to *dura* and *bregma*), then fixed to the skull. Mice were allowed to recover in their home cage for at least 8-10 days before behavioral testing. Forty-five minutes before fear conditioning, intra-CA1, intra-DG or intra-hippocampal bilateral infusion (300 nL or 600 nL per side respectively; 0.1 µL/min) of GluN1 X-link (same as above; 0.2 mg/mL) or its control was performed alone or followed (15 min after) by intra-CA1 bilateral infusion of E2 (10 nM) or vehicle. The *cannulae* were left in place for an additional 2 min before removal to allow diffusion of the drug away from the *cannulae* tips.

Histological control of *cannulae* placements after behavioral testing was used as exclusion criteria. For this purpose, animals were given an overdose of pentobarbital (250 mg/kg) and transcardially perfused with 4% paraformaldehyde. Brains were frozen, cut coronally (60 µm) and counterstained with neutral red (Sigma, France). To check for intra-CA1 or intra-hippocampal GluN1 X-link diffusion, anti-GluN1 was infused 45 min prior to sacrifice and immunohistochemistry on brains sections were performed using only secondary antibody (figures 4B and S1).

Trace fear conditioning

The fear-conditioning task was conducted in a conditioning apparatus (Imetronic, France) described previously (9). During fear conditioning, each animal received five pairings of tone (65 dB, 1 kHz, 30 s) and foot shock (0.3 mA or 0.6 mA as indicated, 50 Hz, 1 s) (context A, figure 4A). Independent groups of mice were trained either with a 20 s interval between the tone and the shock (20 s; *trace* condition) or with the 2 stimuli contiguous (0 s; *delay* condition) (12). The retention of the tone- and context-shock associations acquired during conditioning was tested by re-exposure to the tone alone in a dark and unknown chamber (context B, figure 4A) and to the conditioning context alone (24 h and 26 h post-conditioning, respectively, figure 4A).

At all stages of the experiment, freezing behavior, defined as a lack of all movement except for respiratory-related movements was used as an index of fear responses (13). Animals were

continuously video-recorded and the percentage of time spent freezing was measured by an observer blind of experimental groups. Sample size (n=16 mice/experimental group, in order to obtain at least 9-12 animals after surgery, intra-hippocampal infusions and behavioral procedures) was mainly based on previous studies using similar experimental procedures (9). Histological control of *cannulae* placements after behavioral testing was used as exclusion criteria.

Object location task

The apparatus consists of an open field arena (40x40x40cm) made of white floor and blue acrylic walls. The arena is digitally divided into "zones" to identify the objects and their boundaries (2 cm radius). The objects consist in LEGO blocks (3.5 cm X 3.5 cm X 6 cm) placed in the corners (7.5 cm from walls). An infrared-sensitive camera (Panasonic) was mounted above the chamber and was connected to the video input of the behavioral tracking software (Ethovision XT11, Noldus, The Netherlands) that tracked the animal's position during experimental trials. The software acquired the coordinates of the nose and the body center, which was facilitated by the high contrast between the animals' black coat at the white background. The arena is cleaned with mild detergent disinfectant (Phagospray DM, Christeyns, France) solution and dried in between each subject so as to eliminate any potential odor cues left by previous subjects.

The object location task was performed as described previously (14) with minor modifications. On the first day of the novel object location task (*acquisition*, figure 5A), the mouse is placed into the center of the arena and allowed to freely explore the arena containing the two identical objects placed at adjacent northern locations of the arena. The behavior is recorded for 10 min and analyzed using the tracking software. General locomotor activity was assessed as total track length and was analyzed to confirm that there is no preference for one object over another (table S1). After 24 h, one object (A, non-displaced object, NDO) is placed to its former location, while the other object (A', displaced object, DO) is placed in a new location (southeast corner) of the same arena (figure 5A). The same mouse is returned to the arena and time spent exploring each object is recorded for 3 min and the time spent investigating each of the objects is measured (time spent with nose point to the

objects and in the proximity of the objects). A location index is calculated by dividing the amount of time spent exploring both the DO and NDO divided by the amount of time spent exploring both objects ((Time DO)/(Time NDO + Time DO) and (Time NDO)/(Time NDO + Time DO), respectively), such that mice were successful at the task if they spent significantly more time than chance (0.5) exploring the DO.

Statistics

All quantitative data are expressed as mean±sem. For *in vitro* studies, comparisons between 2 experimental groups were performed using Student's t test or Mann Whitney test, while comparisons between several experimental groups were performed using one way ANOVA statistical analyses followed by *post-hoc* Student's t tests. For QD tracking, the diffusion coefficients D are reported per group as the median±25-75%. Comparisons between groups for D were performed using Mann Whitney test followed by Dunn's Multiple Comparison test (group comparison). For electrophysiology recordings and behavioral data, statistical analyses performed were one or two-way ANOVA, with Bonferroni multiple comparisons or *post-hoc* Student's *t* tests (as detailed in figure legends). Values of $p<0.05$ were considered significant for comparisons and statistical comparisons are indicated as *, ** and *** for $p<0.05$, $p<0.01$ and $p<0.0001$, respectively.

Supplemental Results

To demonstrate the implication of hippocampal surface NMDAR trafficking in NMDAR-dependent associative temporal and contextual memories, we used the *trace* fear conditioning procedure. GluN1 X-link infusion in the whole dorsal hippocampus before conditioning (Figures S1A-B) impairs acquisition of fear conditioning (figure S1C) and both retention of temporal and contextual associative memories (figures S1D-E).

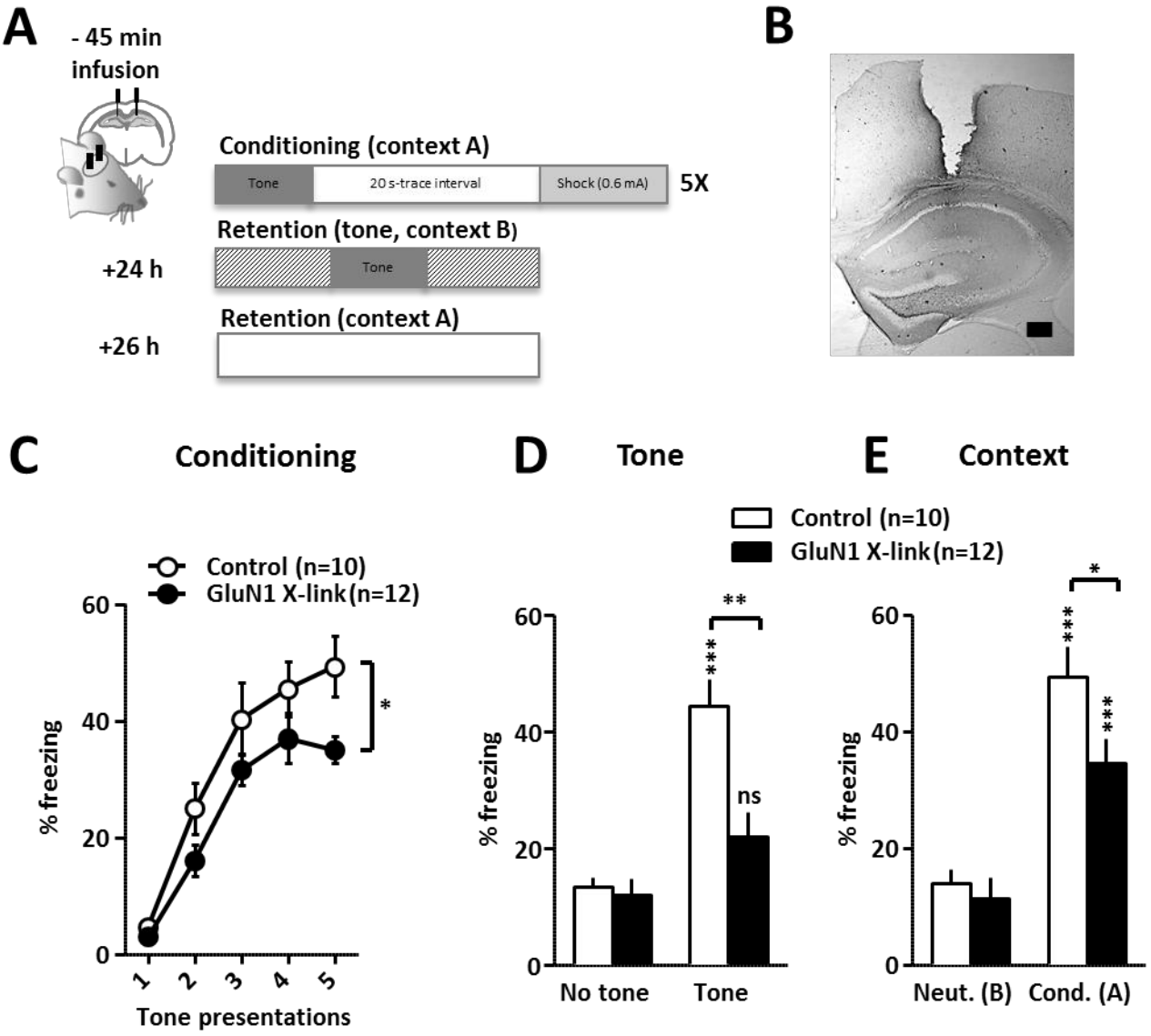

Figure S1. Reduction of NMDAR surface dynamics in the whole dorsal hippocampus impairs acquisition and retention of both temporal and contextual associative memories. (A) Schematic representation of the experimental procedure. Bilateral intra-hippocampal infusions (GluN1 X-link/control, 600 nL per side) were performed 45 min before *trace* fear conditioning (five pairings of tone (65 dB, 1 kHz, 30 s) and foot shock (0.6 mA, 50 Hz, 1 s) with a 20 s interval. Retention of temporal and contextual fear memories, respectively based on a 20 s *trace* tone-shock association and a context-shock association, were measured during re-exposure to the tone alone in a neutral context (context B, tone, 24 h after conditioning) and to the conditioning context (context A, context, 2 h after tone test). **(B)** Representative photography showing location of intra-hippocampus *cannulae*

and the extent of GluN1 X-link diffusion 45 min after infusion in living mice and revealed with only secondary antibody (Scale bar=250µm) **(C) Conditioning:** GluN1 X-link slightly impairs acquisition of *trace* fear conditioning. Even though time spent freezing increases over repeated tone presentations in both groups, freezing level reached at the end of conditioning is significantly reduced by pre-conditioning hippocampal infusion of GluN1 X-link (*Tone repetition*: $F_{4,80}$=54.21 p<0.0001; *Treatment* $F_{1,20}$=0.16; p=0.0231 and *Interaction*: $F_{4,80}$=1.03; p=0.3992) **(D-E) Retention:** GluN1 X-link impairs both the 24 h retention of fear memory based on a temporal association (**D, Tone:** *Tone*: $F_{1,40}$=31.77; p<0.0001; *Treatment:* $F_{1,40}$=10.91; p=0.002; *Interaction*: $F_{1,40}$=8.31 p=0.0063) and contextual association (**E, Context:** *Context*: $F_{1,40}$=53.17; p<0.0001; *Treatment*: $F_{1,40}$=4.81; p=0.0341 and *Interaction*: $F_{1,40}$=2.36; p=0.1323). All graphs show mean±sem of percent of time spent freezing (% freezing); n=numbers of animals. Statistical comparisons to control condition or within experimental groups are indicated by *, ** and *** for p<0.05, p<0.01 and p<0.001, respectively (two-way ANOVA and Student's t test *post-hoc comparisons*).

To further investigate the implication of surface NMDAR trafficking in NMDAR-dependent associative temporal and contextual memories in different subfields of the hippocampus, we performed GluN1 X-link infusion in the Dentate Gyrus (DG) before the *trace* fear conditioning procedure. Reduction of NMDAR surface dynamics in the DG has no effect on acquisition of fear conditioning (*Tone repetition*: $F_{4,64}$=49.3; p<0.0001; *Treatment* $F_{1,16}$=0.16; p=0.69 and *Interaction*: $F_{4,64}$=0.24; p=0.91) and does not impair temporal (*Tone*: $F_{1,32}$=20.4; p<0.0001; *Treatment:* $F_{1,32}$=0.13; p=0.7161; *Interaction*: $F_{1,32}$=0.78; p=0.3840) and contextual (*Context*: $F_{1,32}$=16.1; p<0.0001; *Treatment*: $F_{1,32}$=0.21; p=0.6488 and *Interaction*: $F_{1,32}$=0.02; p=0.8792) associative memories .

To emphasize the selectivity of hippocampal CA1 surface NMDAR trafficking requirement for associative temporal memory, we used the object location task, which depends on hippocampal CA1 (14) but has no demand on temporal memory. GluN1 X-link infusion in the dorsal CA1 before *acquisition* phase does not impair acquisition and retention of spatial memory (table S1).

Table S1 depicts the effects of GluN1 X-link or control infusions in the dorsal CA1 on the locomotor activity (total track length) and exploration of both objects during the a*cquisition* and the *test* phases. During the *test* phase, both experimental groups exhibited a higher time exploring DO compared to NDO (shaded lines). However, total track length and time spent exploring both objects did not differ between groups both during *acquisition* and *test* phases.

Table S1: Behavioral parameters evaluated during *acquisition* and *test* phases of the object location task in mice submitted to control and GluN1 X-link infusions in dorsal CA1 before *acquisition* phase.

	Control (mean±SEM)	**GluN1 X-link (mean±SEM)**
Total track length (cm) during *acquisition*	**1373*±68.8***	***1374±66.5***
Total track length (cm) during *test* phase	**1151±64.9**	**1094±60.8**
Time exploring object A/*object A+boundary* **(s) during *acquisition***	**2.6±0.5** / *9.32±1.4*	**2.7 ±0.5** / *10.4±1.2*
Time exploring object A'/*object A'+boundary* **(s) during *acquisition***	**2.8±10.7** / *9.9±1.0*	**2.2 ±0.5** / *9.9±1.5*
Time exploring NDO(A)/*NDO(A)+boundary* **(s) during *test* phase**	**1.9±0.4** / *9.5±1.1*	**2.5±0.6** / *13.0±2.8*
Time exploring DO(A')/*DO(A')+boundary* **(s) during *test* phase**	**5.8±2.4** / *18.5±2.6*	**4.4±1.1** / *19.1±3.3*

Supplemental References

1. Banker GA, Cowan WM (1977): Rat hippocampal neurons in dispersed cell culture. *Brain Res*. 126:397-342.

2. Groc L, Heine M, Cognet L, Brickley K, Stephenson FA, Lounis B, et al. (2004): Differential activity-dependent regulation of the lateral mobilities of AMPA and NMDA receptors. *Nat Neurosci*. 7:695-696.

3. Groc L, Heine M, Cousins SL, Stephenson FA, Lounis B, Cognet L, et al. (2006): NMDA receptor surface mobility depends on NR2A-2B subunits. *Proc Natl Acad Sci U S A*. 103:18769-18774.

4. Ehlers MD, Heine M, Groc L, Lee MC, Choquet D (2007): Diffusional trapping of GluR1 AMPA receptors by input-specific synaptic activity. *Neuron*. 54:447-460.

5. Dupuis JP, Ladepeche L, Seth H, Bard L, Varela J, Mikasova L, et al. (2014): Surface dynamics of GluN2B-NMDA receptors controls plasticity of maturing glutamate synapses. *Embo J*. 33:842-861.

6. Groc L, Choquet D, Chaouloff F (2008): The stress hormone corticosterone conditions AMPAR surface trafficking and synaptic potentiation. *Nat Neurosci*. 11:868-870.

7. Heine M, Groc L, Frischknecht R, Beique JC, Lounis B, Rumbaugh G, et al. (2008): Surface mobility of postsynaptic AMPARs tunes synaptic transmission. *Science*. 320:201-205.

8. Han J, Kesner P, Metna-Laurent M, Duan T, Xu L, Georges F, et al. (2012): Acute cannabinoids impair working memory through astroglial CB1 receptor modulation of hippocampal LTD. *Cell*. 148:1039-1050.

9. Kaouane N, Porte Y, Vallee M, Brayda-Bruno L, Mons N, Calandreau L, et al. (2012): Glucocorticoids can induce PTSD-like memory impairments in mice. *Science*. 335:1510-1513.

10. Etchamendy N, Enderlin V, Marighetto A, Vouimba RM, Pallet V, Jaffard R, et al. (2001): Alleviation of a selective age-related relational memory deficit in mice by pharmacologically induced normalization of brain retinoid signaling. *J Neurosci*. 21:6423-6429.

11. Mingaud F, Le Moine C, Etchamendy N, Mormede C, Jaffard R, Marighetto A (2007): The hippocampus plays a critical role at encoding discontiguous events for subsequent declarative memory expression in mice. *Hippocampus*. 17:264-270.

12. Misane I, Tovote P, Meyer M, Spiess J, Ogren SO, Stiedl O (2005): Time-dependent involvement of the dorsal hippocampus in trace fear conditioning in mice. *Hippocampus*. 15:418-426.

13. Fanselow MS (1980): Conditioned and unconditional components of post-shock freezing. *Pavlov J Biol Sci*. 15:177-182.

14. Assini FL, Duzzioni M, Takahashi RN (2009): Object location memory in mice: pharmacological validation and further evidence of hippocampal CA1 participation. *Behav Brain Res*. 204:206-211.

MS number: BPS-D-15-00271

In this issue

Hippocampal glutamatergic receptors (GluNR) are critically involved in synaptic plasticity and memory. Recent discovery that GluNR can rapidly move in and out the synapse at the neuronal surface has raised the question of whether this surface trafficking sustains GluNR physiological functions. Indeed, GluNR surface trafficking and its modulation by the sex hormone estradiol is a cellular mechanism critical for a major component of episodic memory. This discovery could change our understanding of GluNR signaling implicated in various neuropsychiatric and aging-related cognitive disorders.